J Sol-Gel Sci Technol (2012) 61:620–627
DOI 10.1007/s10971-011-2668-4

ORIGINAL PAPER

ZnO:Al thin films used in ZnO: Al/p-Si heterojunctions

N. Baydogan · O. Karacasu · H. Cimenoglu

Received: 12 April 2011 / Accepted: 22 December 2011 / Published online: 10 January 2012

Abstract Al-doped n-ZnO/p-Si heterojunctions were fabricated using a sol–gel dip coating technique at 700 °C, in a nitrogen ambient. The structural, optical, and electrical properties of ZnO:Al thin films, and the heterojunction properties of ZnO:Al/p-Si were investigated with respect to the effects of Al doping concentration. Hexagonal nanostructured ZnO: Al thin films with a 1.2% and a 1.6 at.% Al concentration exhibited high optical transmittance in visible ranges. Electrical resistivity changed with respect to Al doping concentration, and minimum resistivity was detected at a 1.2 at.% Al concentration. The ZnO:Al/p-Si heterojunction properties were analysed using current–voltage (I–V) measurements at four different Al concentrations, ranging from 0.8 to 1.6 (at.%). The ZnO:Al/p-Si heterojunctions exhibited diode-like rectifying behaviour. Under UV illumination, the photoelectric behaviour observed for the ZnO:Al/p-Si heterojunctions was diode.

Keywords Coating process · Heterojunction · Sol–gel · Thin films

1 Introduction

In recent years, transparent conducting oxide (TCO) films have aroused much interest. With their outstanding properties such as high optical and electrical properties, doping suitability, being non-toxic, its high resistivity control, its high chemical, mechanical, and thermal stability, as well as being abundant in nature, and cost effective, Zinc Oxide (ZnO) films are good candidates for TCO films [1–5]. Due to these superior properties, ZnO is a good choice for electronic or optoelectronic applications like antireflection coatings, transparent electrodes in solar cells, thin film gas sensors, varistors, light emitting diodes, nanolasers heterojunctions, etc. [5–12]. Various techniques such as sputtering, chemical vapour deposition, spray pyrolsis, sol–gel, etc. [13] were used to fabricate ZnO films. Compared to ZnO films, Al-doped ZnO (ZnO:Al) films have lower resistivity and better stability [14]. The deposition of ZnO films on p/n type substrates generates heterojunctions used for the fabrication of solar cells and optoelectronic devices [15, 16]. The major advantage of these heterojunctions is combining the large binding energy of ZnO thin films, and the economy of Si substrates [16].

This study contributes to the field as there are not many existing studies regarding the heterojunction properties of ZnO:Al/p-Si, produced using a sol–gel dip coating technique due to the increase of Al concentration. The ZnO:Al/p-Si heterojunctions generated from 0.8 to 1.6 (at.%) Al concentrations have as yet to be reported for the utilisation in rectifier diodes of electronic devices controlled by spherical forms of ZnO:Al nanocrystallites. The ZnO:Al thin films with four different Al concentrations are prepared from colloidal suspensions, to control the nature of nanospheres in the ZnO:Al texture, because the colloidal solution is utilised as a template to control the particle shape. This paper presents novel data on the ideality factor, the saturation current, the rectification ratios, and the photoelectric behaviours of the ZnO:Al/p-Si heterojunctions. The structural, optical, and electrical properties of

N. Baydogan (✉)
Energy Institute, Istanbul Technical University, Maslak, 34469 Istanbul, Turkey
e-mail: dogannil@itu.edu.tr

O. Karacasu · H. Cimenoglu
Materials Division, Metallurgical and Materials Engineering Department, Istanbul Technical University, Maslak, 34469 Istanbul, Turkey

ZnO:Al thin films were also investigated in order to characterise ZnO:Al thin films.

2 Experimental study

In this study, ZnO:Al thin films, with 0.8, 1.0, 1.2 and 1.6 at.% Al concentrations, were fabricated on p-type silicon (100) wafer substrates, using the sol–gel dip coating technique. Optical properties and film resistivity of ZnO:Al thin film were investigated on borosilicate glass substrates. After immersing the substrates in colloidal suspension, the samples were preheated at 400 °C for 10 min. This procedure was repeated four times. After the final preheating, the samples were annealed at 700 °C, for 1 h, in a nitrogen ambient.

2.1 Preparation of solutions and deposition of films

A 50-ml aqueous solution was prepared. The solution consisted of absolute ethanol, as the solvent material, and zinc acetate dehydrate $Zn(CH_3COO)2{\cdot}2H_2O$), 99.5% purity), as the starting material, and the molar concentration of the zinc was 0.5 M. The diethanolamin $DEA(CH_2CH_2OH)_2$ was added as a stabiliser, and a measured amount of Al nitrate nano hydrate $Al(NO_3)_3{\cdot}9H_2O$ (extra purity) was added as the dopant source to obtain 0.8–1.0–1.2–1.6 at.% Al ratio (Rm = Al/Zn).

The molar ratio of DEA to Zinc acetate-dehydrate was maintained at 1.0. Then the resulting mixture was stirred, with a magnetic stirrer, at 60 °C, for 1 h to form a clear, transparent, and homogeneous solution. After cooling, the solutions were aged at room temperature for 1 day. The humidity level of the ambient was fixed at 43% using a dehumidifier to protect the solution quality during the preparation of the solution and the dip coating processes. The solutions were kept at 5 °C to prevent precipitation and to extend the life of the solution.

Differential thermal and thermo gravimetric analyses (DTA/TGA) were performed using Perkin Elmer Diamond TG-DTA thermal analyses equipment in order to investigate the thermal behaviours of ZnO:Al thin films. Thermal analyses were performed in an air atmosphere with a 10 °C/min heating and cooling rate from room temperature to 1,200 °C, and from 1,200 °C to room temperature, respectively. According to the analyses, the ZnO:Al indicated an endothermic peak up to 420 °C, which helps to define the pre-heating temperature as 400 °C, made to evaporate the solvent and organic residuals. A noticeable mass loss (~70%) was observed at ~520 °C. The annealing temperature, which is set for the crystallisation of deposited films, was defined as 700 °C in order to obtain high-quality crystallisation [17].

The readily-prepared ZnO:Al solutions were deposited on 10 × 30 mm p-type silicon wafers (100) and 35 × 35 mm borosilicate using a sol–gel dip coating technique with a KSV dip coater LMX2. After cleaning the substrates were dipped and drawn into the solution at a rate of 200 mm/min, and were kept in the solution for 5 s. The films were then pre-heated at 400 °C for 10 min in an oxygenated ambient. This application was repeated four times. The four layered thin films were annealed at 700 °C, for 1 h, in the nitrogen ambient. The pressure of the nitrogen gas was 1,013.25 mbar and its flow rate was 30 L/h [17].

Structural characteristics of the film were analysed by gamma transmission method [18] and the effects of Al concentration on the ZnO film structure were examined clearly due to the accuracy and reproducibility of this method. The linear absorption coefficient of the ZnO:Al thin film was examined using the certified point gamma source of a Cs-137 radioisotope with a 0.832 μCi, in monochromatic conditions at 0.662 MeV. When energetic gamma photons pass through the matter, they become scattered and absorbed [19], principally by photoelectric and Compton processes. The intensity of a collimated beam of mono-energetic photons, with an initial intensity I_o, is reduced to I_x, after travelling through the thickness x of the matter, according to the Bouger-Lambert–Beer law [18, 20]

$$I_x = I_o \exp(-ux) \quad (1)$$

where, u is the linear absorption coefficient of the film concerned. u is a quantity that depends on the energy of the photons in the beam, and on the probability of the interaction between those photons and the molecules that constitute the matter, through which they pass.

2.2 Characterisation of ZnO:Al thin films and ZnO:Al/P–Si heterojunctions

In this study, the structural, optical, and electrical behaviours of ZnO:Al films, and the heterojunction properties of ZnO:Al/p-Si, were investigated using an X-Ray diffractometer, a scanning electron microscopy, a surface profilometer, a UV/VIS spectrophotometer, a four point resistivity probe, and a semiconductor characterisation system.

The X-Ray diffraction patterns of the thin films were taken using a GBC-MMA X-Ray diffractometer with a 1.54 Å-wavelength Cu Kα radiation at room temperature. The diffractometer was operated at 35 kV and 28.5 mA, with energy of 1 kWatt, and a 2 deg/min constant scan rate was used to collect 2θ data between 20° and 60°. By means of a JEOL 6335F Scanning Electron Microscope (SEM) with a 20 kV accelerating voltage SEM images of the

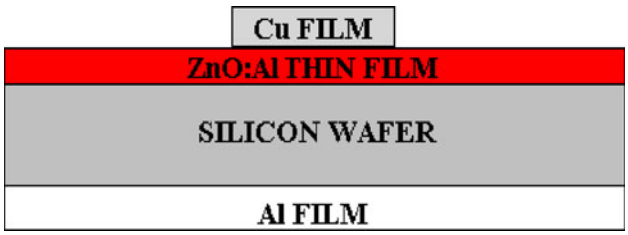

Fig. 1 A schematic diagram of the ZnO:Al/Si heterojunction

surface of the thin film were taken. The thickness measurements were carried out using a Veeco Dektak- 6 M surface profilometer. The thickness difference between coated and uncoated parts of the films constitutes the basis of measurement. For investigating optical properties of the films, optical transmittance and reflectance measurements were utilised. Optical measurements were performed in a wavelength range from 192.5 to 900 nm, using a T80 UV/VIS Spectrophotometer. The electrical resistivity of ZnO:Al thin films were measured using a Four Point Resistivity Probe, with a Mounting Stand (SIGNATONE).

The current–voltage characteristics of the p-n junctions, produced using a sol–gel dip coating, were investigated, as well. Heterojunctions were fabricated using the configuration Cu/ZnO:Al/Si/Al. A Univex 450 Thermal Evaporator was used in preparing the samples, for investigation of current–voltage characteristics. After the deposition of the ZnO:Al thin film, the ohmic back contact of the Si wafer was fabricated by thermally evaporating Al ($\sim$0.8 µm-thick), while the other ohmic contact was fabricated with a Cu-grid ($\sim$0.8 µm-thick), through a mask on the front side. During the thermal evaporation, the vacuum level was $\sim 6.5 \times 10^{-6}$ Pa. The areas of the Al and Cu electrodes were 0.25 and 0.07 cm^2, respectively. Figure 1 illustrates the schematic diagram of ZnO:Al/Si heterojunctions. Additionally, direct current voltage (DC) in a range between -20 and $+20$, at room temperature, under dark and light (xenon lamp 100 mW/cm^2) conditions via a Keithley 4200 Semiconductor characterisation system (SCS) was used to analyse current voltage characteristics.

3 Result and discussion

3.1 Structural properties

ZnO:Al thin films having thicknesses of about 280 $\pm$ 5 nm were deposited on the substrates. Figure 2 illustrates the X-ray diffraction patterns of the films on borosilicate glass substrates. The wurtzite structure of all XRD peaks was identified. The (100), (002), (101), (110) and (103) diffraction peaks are observed at four different Al concentrations such as 0.8, 1.0, 1.2 and 1.6 at.% Al.

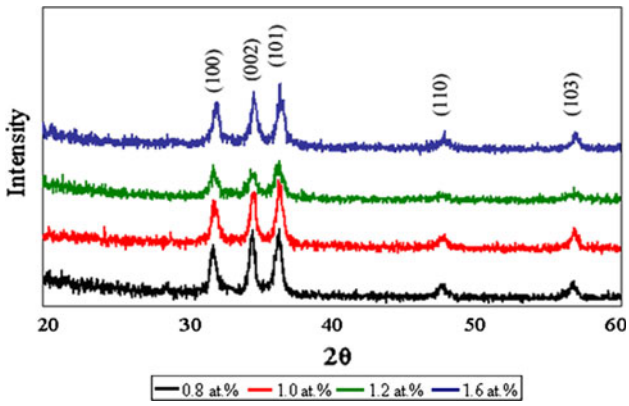

Fig. 2 The X-Ray diffraction patterns of ZnO:Al thin films with an increased Al concentration

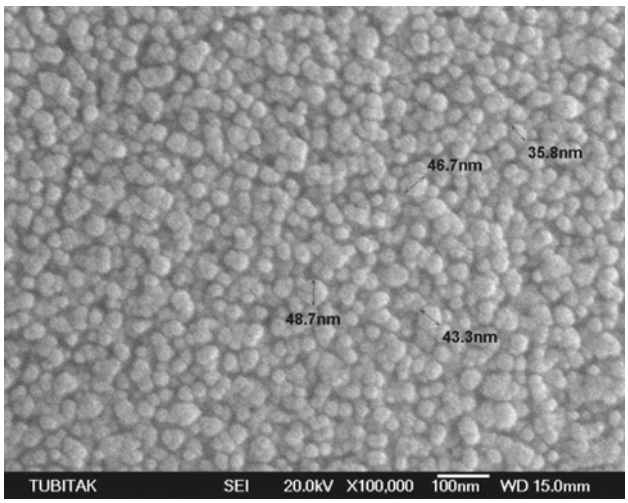

Fig. 3 The SEM image of the surface of ZnO:Al thin film with a 1.2 at.% Al concentration

Representative SEM image of the ZnO:Al film at 1.2 at.% Al concentration is illustrated in Fig. 3. SEM image of ZnO:Al film annealed at 700 °C in the nitrogen atmosphere magnified by 100.000× magnification. In the general films exhibited spherical morphology on the surface of the ZnO:Al film. Nano-spherical particle sizes of the films varied in the range between approximately 35.8 and 48.7 nm.

Figure 4 illustrates the changes in linear absorption coefficients of the ZnO:Al films with respect to the Al doping concentration. Increase of Al (at.%) concentration from 0.8 to 1.6 has accompanied by an increase of the linear absorption coefficient. Since the thicknesses of the examined ZnO:Al films did not change significantly with respect to Al concentration, increase in the linear absorption coefficient can be attributed to the enhancement of density with the increase of Al (at.%) in the film.

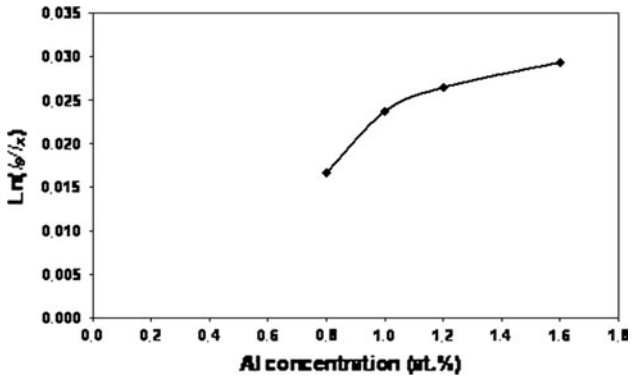

Fig. 4 The changes in the linear absorption coefficients of the ZnO:Al thin films with an increased Al concentration

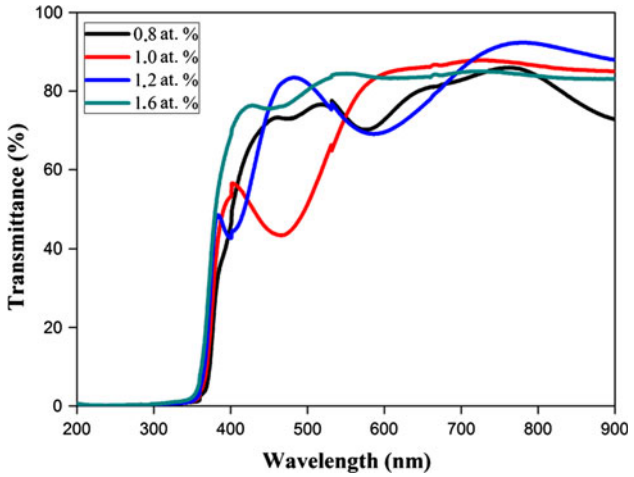

Fig. 5 The optical transmittance spectra of ZnO:Al films at different Al concentrations

3.2 The optical properties

Figure 5 illustrates the transmittance spectrum of the examined ZnO:Al thin films. Sharp absorption edges were observed at ~370 nm in ultraviolet (UV) range. The optical band gap widens with the increase in Al concentration from 0.8 to 1.6 at.%. The Moss-Burstein shift [7] explains the reason behind why these band gaps widen with the increase in the Al concentration. According to the Moss–Burstein theory, the donor electrons occupy bottom states of the conduction band in highly doped zinc oxide films [21]. The optical gap is defined as the minimum energy needed to excite an electron from the valence band to the conduction band [22]. In general, the blue shift of the absorption onset of Al doped nano-crystalline films, is associated with the increase in the carrier concentration, blocking the lowest states in the conduction band, commonly known as the Burstein–Moss effect [4]. Figure 6 illustrates the plots of $(\alpha h\nu)^2$ versus hν, drawn for ZnO:Al

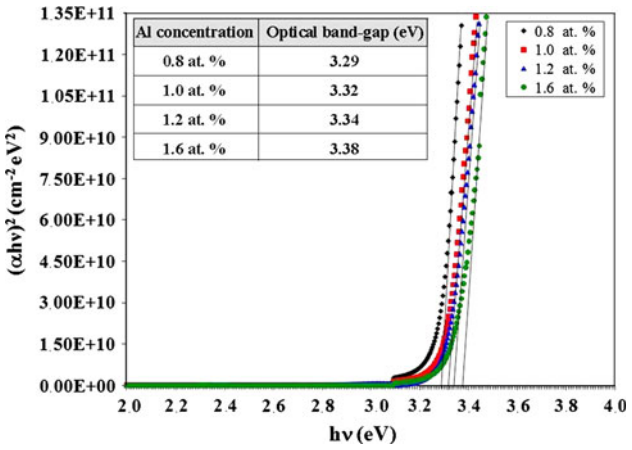

Fig. 6 The changes in the optical band gap of the ZnO:Al films with different Al concentrations

thin films, where the α and hν values are calculated according to Eq. 3 [23–26]. Thus it may write

$$\alpha n_0 \hbar\omega \sim (\hbar\omega - E_0)^n \quad (2)$$

$$\alpha = A(h\gamma - E_0)^{1/2} \quad (3)$$

where, E_0, is the optical band gap, and n_0, is the refractive index in the relation (2) [23, 24]. In an allowed direct transition, α is given in Eq. 3. A is a constant [25, 26]. For this study, the n value was determined as 1/2 for $(\alpha h\nu)^{1/n}$. From the plot, the optical band gap was determined by extrapolating the linear portion of the graph to $h\nu = 0$. It is determined that there is an allowed direct transition of $(\alpha h\nu)^2$ for ZnO:Al film. It is obvious that the changes in the optical band gap portray a blue shift with the increase in the Al doping concentration.

3.3 The electrical properties

Figure 7 illustrates variation of resistivity of the examined ZnO:Al films with respect to Al concentration. The minimum resistivity value was obtained at 1.2 at.% Al concentration by using four point *probe*. It is suggested that the decrease in the resistivity together with the increase in Al concentration until 1.2% is due to the electrons that come from the donor Al^{3+} ions, incorporated as substitution Zn^{2+}cation sites, or in interstitial position. Further increase in Al concentration produces a rise in the resistivity probably due a diminution in the carrier mobility because of the excess of Al [3].

3.4 The heterojunction properties of ZnO:Al/p-Si

The current that passes through a diode, as a function of voltage, is expressed by the diode equation. Equation 4 illustrates the ideal diode law [16].

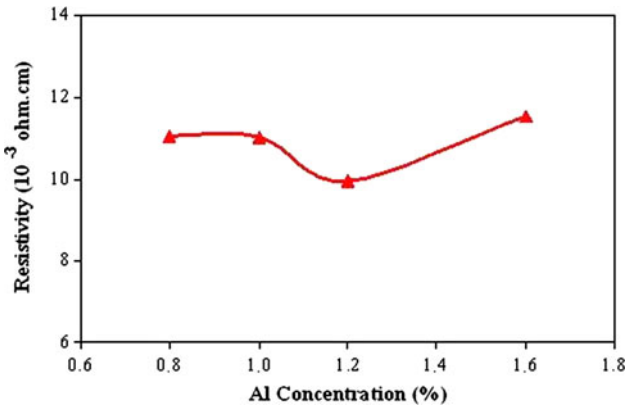

Fig. 7 The resistivity of Al-doped ZnO thin film, annealed at 700 °C, as a function of Al concentrations

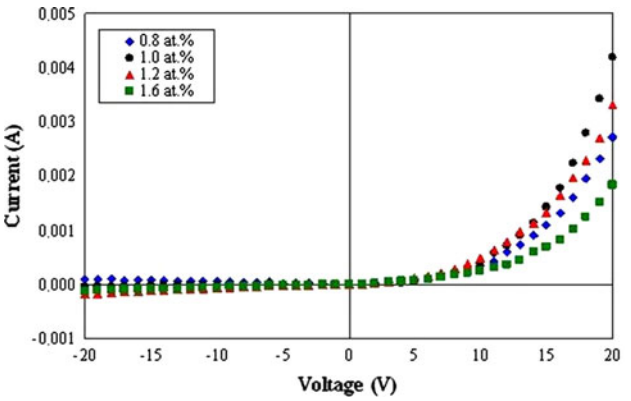

Fig. 8 The measured current–voltage characteristics of ZnO:Al/p-Si heterojunctions at different Al concentrations, in the dark

$$I = I_o(e^{(qV/nkBT)} - 1) \quad (4)$$

where, I, is the net current flowing through the diode; I_0, is the dark saturation current, (the diode leakage current density in the absence of light); V, is the applied voltage through the diode; q, is the absolute value of electron charge (1.6×10^{-19} C); n, is the ideality factor; k_B, is the Boltzmann's constant (1.38×10^{-23} J/K); T, is the absolute temperature [16]. n, the ideality factor is obtained in Eq. 5. The "dark saturation current" (I_0), is a parameter that differentiates one diode from another. I_0, is a measure of the recombination in a device. A diode with a larger recombination will have a larger I_0. The ideality

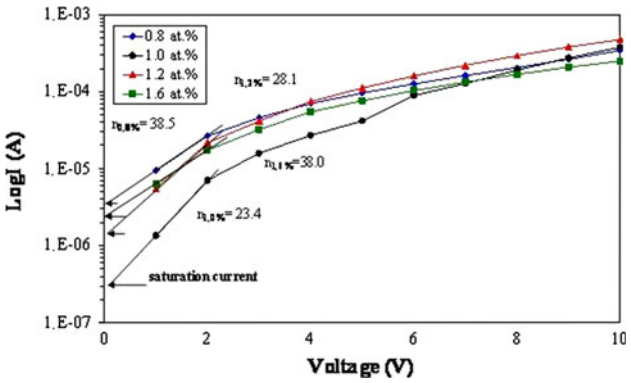

Fig. 9 The semi log I–V characteristics of ZnO:Al/p-Si heterojunctions at different Al concentrations, in the dark

factor (n) of heterojunctions can be determined from the slope of the straight line region of the forward bias log I–V characteristics [16].

$$n = q/(k_B T)(dV/dLn(I)) \quad (5)$$

Figure 8 illustrates the current–voltage characteristic of the ZnO:Al/p-Si heterojunctions, measured at room temperature, in the dark. The ZnO:Al heterojunctions, annealed at 700 °C, in a nitrogen ambient, had different Al concentrations ranging from 0.8 to 1.6 at.%. While in forward bias, the current passing through the heterojunctions, changed with the applied voltage, in reverse bias, the current passing through the heterojunctions showed no significant change with the change in voltage. The similarity of the I–V characteristics indicates that a diode forms between the sol–gel prepared ZnO:Al thin films, and the p-Si wafer. Table 1 illustrates that diodes show rectifying behaviour with the rectification ratio, I_F/I_R, (I_F and I_R are forward and reverse current respectively) values at a ± 20 V bias voltage. The most conductive and rectifier ZnO:Al/p-Si heterojunction is determined with a 1.0 at.% Al concentration in the Cu/ZnO:Al/Si/Al configuration. The I–V curve of the ZnO:Al/p-Si heterojunction with a 0.8 at.% Al concentration occurs in the positive region of the reverse bias, in the second quadrant. This leads to the deviation of diode characteristics from those of the ideal diode. Figure 9 illustrates the dependence of the forward current in logarithmic scale with the change in Al concentration. The ideality factor of the ZnO:Al/p-Si heterojunction is determined from the slope of the straight line region of the forward bias log I–V

Table 1 I_0, n, and I_F/I_R values of ZnO:Al/p-Si heterojunctions, and measured current values at −10 V in the dark and light for heterojunctions with different Al concentrations

Al concentration %	Log I_0	n	I_F/I_R	$I_{dark\ at\ -10V}$	$I_{light\ at\ -10V}$
0.8	3.5×10^{-6}	38.5	26.80	-48.9026×10^{-6}	-2.7206×10^{-3}
1.0	3.0×10^{-7}	23.4	100.06	-14.5837×10^{-6}	-2.1496×10^{-3}
1.2	1.5×10^{-6}	28.1	18.59	-65.3068×10^{-6}	-1.9634×10^{-3}
1.6	2.5×10^{-6}	38.0	14.21	-50.0536×10^{-6}	-2.1689×10^{-3}

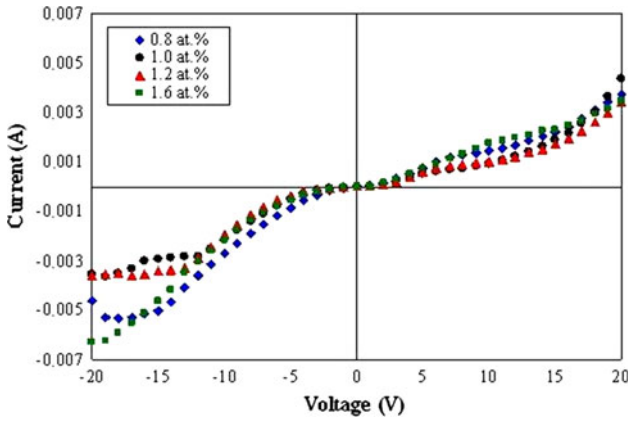

Fig. 10 The measured current–voltage characteristics of ZnO:Al/p-Si heterojunctions at different Al concentrations, under the light

characteristics. Figure 10 illustrates the current–voltage characteristics of the ZnO:Al/p-Si heterojunction, measured at room temperature, illuminated by a UV light source (xenon lamp 100 mW/cm^2); hence, determining the photoelectric behaviours. UV illumination improved the current passing through the ZnO:Al/p-Si heterojunctions in the forward bias. In reverse bias, the photocurrent, caused by the xenon lamp, was significantly larger than the current under dark conditions. ZnO:Al films were highly transparent as ~80 T (%) in the visible region, and visible light passing through the ZnO:Al films. When the semi-logarithmic forward-biased curves in Fig. 10 are fitted to the standard diode equation given in Eq. 4, the ideality factors of the diodes, fabricated in a nitrogen ambient, at 700 °C are as illustrated in Table 1. It is determined that heterojunctions with 1.0 and 1.2 at.% Al concentrations, declare lower ideality factors (n) than that of heterojunctions with 0.8 and 1.6 at.% Al concentration. Table 1 illustrates that the samples with 1.0 and 1.2 at.% Al concentrations had the considerable increase in the initial slant of the forward current in logarithmic scale LogI_0, with a decrease in the ideality factor of the ZnO:Al/p-Si heterojunction than the samples at other Al concentrations. The ideality factors found in our research are similar to the ideality factors stated in various works in literature [27, 28].

Figure 11 illustrates the current density–voltage characteristics of ZnO:Al/p-Si heterojunctions at four different Al concentrations, measured at room temperature, both under dark conditions, and under the illumination of a UV light source (xenon lamp 100 mW/cm^2). Table 1 also illustrates the values of the current flow through the ZnO:Al/p-Si heterojunctions, in the dark and under UV illumination, in reverse bias. The current flows increase under UV illumination for each Al concentration. A high photocurrent is obtained under reverse bias, due to the crystalline quality of ZnO:Al structure (in XRD results). The results show that the determined current–voltage

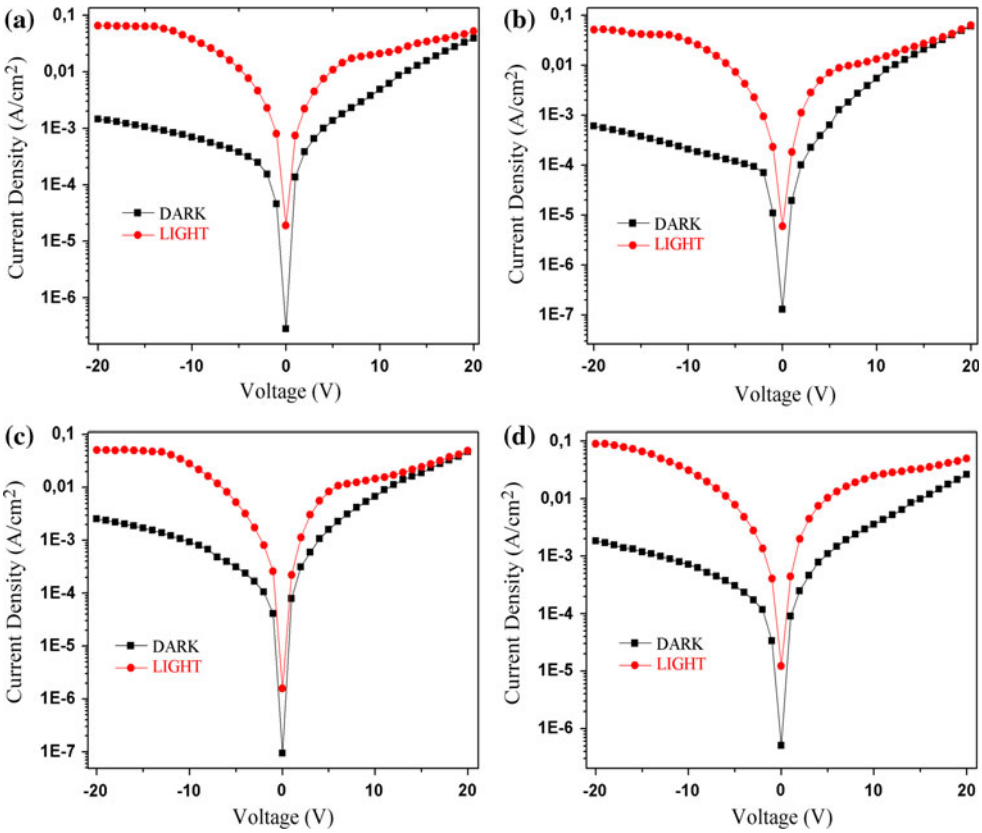

Fig. 11 The measured current density–voltage characteristics of ZnO:Al/p-Si heterojunctions at **a** 0.8 at.%, **b** 1.0 at.%, **c** 1.2 at.%, **d** 1.6 at.% Al concentrations annealed

characteristics of the ZnO:Al/p-Si heterojunction in the dark, which demonstrated rectifying behaviour and formation of a diode between ZnO:Al and p-Si. Heterojunctions at 1.0 and 1.2 at.% Al concentrations presented lower ideality factors (n) than ideality factors of heterojunctions at 0.8 and 1.6 at.% Al concentrations. The curves in forward bias have lower values than the values of the curves in reverse bias under dark until 20 V which indicate the formation of the diode for all Al concentration. Besides, the curves in forward bias is lower than the curves in reverse bias under dark and light conditions until 5 V which indicates the formation of a diode for the ZnO:Al/p-Si heterojunction at 1.2 at.% Al concentration.

4 Conclusion

In this study, ZnO:Al films on the substrates were coated using a sol–gel dip coating technique and ZnO:Al films were prepared at 0.8, 1.0, 1.2, and 1.6 at.% Al concentrations. After immersing in a prepared solution, samples were preheated at 400 °C, in air, for 10 min, and then annealed at 700 °C, in the nitrogen ambient, for 1 h. The properties of the ZnO:Al/p-Si heterojunction structure were examined after investigating the structural, optical, and electrical behaviours of the ZnO:Al thin film.

The conclusions drawn according to the results of this study are as following.

(1) ZnO:Al thin films having hexagonal wurtzite crystal structure were deposited on the substares with thickness of about 280 nm. The changes in the linear absorption coefficient due to the increase in Al concentration were clearly examined using a gamma transmission technique; the increase in the Al concentration determined the increase in the linear absorption coefficient of the ZnO:Al thin film.
(2) The optical transmittance of the films varied between 40 and 80% in the visible range, for the Al concentration, ranging from 0.8 at.% to 1.6 at.%. An increase in the Al concentration, led to an increase in the optical band gap. The widening of the optical band gap was detected upon increasing the Al concentration of the films.
(3) The minimum resistivity of the ZnO:Al thin film, on the borosilicate glass substrate, was observed with 1.2 at.% Al concentration.
(4) While in forward bias, the current passing through the ZnO:Al/p-Si heterojunctions changed with the applied voltage, in reverse bias, the current passing through the heterojunctions showed no significant change in the dark. These I–V characteristics of the ZnO:Al/p-Si heterojunctions are similar to the I–V characteristics of a typical diode. Heterojunctions exhibited photoelectric behaviour under light conditions. In forward bias, UV illumination improved the current passing through the ZnO:Al/p-Si heterojunctions. In reverse bias, the photocurrent caused by the illumination was larger than the current passing through in the dark. Lower ideality factors (n) at 1.0 and 1.2 at.% Al concentrations were determined than ideality factors at 0.8 and 1.6 at.% Al concentrations. The initial slant of the forward current increased coınsiderably at the samples with 1.0 and 1.2 at.% Al concentrations while the ideality factors decreased. The changes on I–V characteristics indicates that the increase of Al concentration from 0.8 to 1.2 at.% is assisted the increase on current density slightly.
(5) Consequently, ZnO:Al thin films at 1.0 and 1.2 at.% Al concentrations on the p-Si substrate, annealed at 700 °C, in the nitrogen ambient, are better candidates for using ZnO:Al/p-Si heterojunctions as rectifying diodes in electronic devices.

Acknowledgements This study is supported by TUBITAK, as a research project with a project number 107M545.

References

1. Nunes P, Fortunato E, Tonello P, Braz Fernandes F, Vilarinhob P, Martins R (2002) Effect of different dopant elements on the properties of ZnO thin films. Vacuum 64:281–285
2. Sahay PP, Nath RK (2008) Al doped ZnO thin films as methanol sensors. Sens Actuators B 134:654–659
3. Sahal M, Hartiti B, Ridah A, Mollar M, Mari B (2008) Structural, electrical and optical properties of ZnO thin films deposited by sol–gel method. Microelectron J 39:1425–1428
4. Xu ZQ, Deng H, Li Y, Guo QH, Li YR (2007) Characteristics of Al-doped c-axis orientation ZnO thin films prepared by the sol–gel method. Mater Res Bull 41(2006):354–358
5. Kaid MA, Ashour A (2007) Preparation of ZnO-doped Al films by spray pyrolysis technique. Appl Surf Sci 253:3029–3033
6. Gumus C, Ozkendir OM, Kavak H, Ufuktepe Y (2006) Structural and optical properties of zinc oxide thin films prepared by sprey pyrolysis method. J Optoelectron Adv Mater 8:299–303
7. Wang MS, Lee KE, Hahn HS, Kim EJ, Kim S, Chung JS, Shin EW, Park C (2007) Optical and photoluminescent properties of sol-gel Al-doped ZnO thin films. Mater Lett 61:1118–1121
8. Kluth O, Schöpe G, Hüpkes J, Agashe C, Müller J, Rech B (2003) Modified Thornton model for magnetron sputtered zincoxide film structure and etching behavior. Thin Solid Films 442:80–85
9. Shishiyanu ST, Shishiyanu TS, Lupan OI (2005) Sensing characteristics of tin-doped ZnO thin films as NO_2 gas sensor. Sens Actuators B 107:379–386
10. Suvaci E, Özer İÖ (2005) Processing of textured zincoxide varistors via templated grain growth. J Euro Ceram Soc 25: 1663–1673
11. Saito N, Haneda H, Sekiguchi T, Ohashi N, Sakaguchi I, Koumoto K (2002) Low-temperature fabrication of light-emitting zinc oxide micropatterns using self-assembled monolayers. Adv Mater 14:418–421

12. Huang MH, Mao S, Feick H, Yan H, Wu Y, Kind H, Weber E, Russo R, Yang P (2001) Room-temperature ultraviolet nanowire nanolasers. Science 292:1897–1899
13. Wang M, Zhang L (2009) The influence of orientation on the photoluminescence behavior of ZnO thin films obtained by chemical solution deposition. Mater Lett 63:301–303
14. Lee J, Lee D, Lim D, Yang K (2007) Structural, electrical and optical properties of ZnO:Al films deposited on flexible organic substrates for solar cell applications. Thin Solid Films 515: 6094–6098
15. Breivik TH, Diplas S, Ulyashin AG, Gunnæs AE, Olaisen BR, Wright DN, Holt A, Olsen A (2007) Nano-structural properties of ZnO films for Si based heterojunction solar cells. Thin Solid Films 515:8479–8483
16. Bo H, Quan MZ, Jing X, Lei Z, Sheng ZN, Feng L, Cheng S, Ling S, Yue ZC, Shan YZ, Ting YY (2009) Characterization of AZO/p-Si heterojunction prepared by DC magnetron sputtering. Mater Sci Semicond Process 12:248–252
17. Karacasu O (2010) Nanocrystalline ZnO:Al thin films prepared by sol-gel dip coating technique and ZnO:Al/p-Si heterojunctions, MSc Thesis, Istanbul Technical University
18. Everett S, Malcolme-Lawes DJ (1984) Gamma photon attenuation measurement as a technique for monitoring liquid composition. J Autom Chem 6(2):84–87
19. Khanna A, Bhatti SS, Singh KJ, Thind KS (1996) Gamma-ray attenuation coefficients in some heavy metal glasses at 662 keV. Nucl Instrum Methods Phys Res B 114:217–220
20. Singh K, Singh H, Sharma V, Nathuram R, Khanna A, Kumar R, Bhatti SS, Sahot HS (2002) Gamma-ray attenuation coefficients in bismuth borate glasses. Nucl Instrum Methods Phys Res B 194:1–6
21. Lee KE, Wang M, Kim EJ, Hahn SH (2008) Structural, electrical and optical properties of sol–gel AZO thin films. Curr Appl Phys 9:683–687
22. Serneleus BE, Berggren KF, Jin ZC, Hsmberg I, Granqvist CG (1988) Band gap tailoring of ZnO by means of heavy Al doping. Phys Rev B 37:10244–10248
23. Mott NF, Davis EA (1979) Electronic processes in non-crystalline materials, 2nd edn. Clarendon Press, Oxford
24. Smith RA (1978) In: Arrowsmith JW (ed) Semiconductors, 2nd edn. Cambridge University Press, Bristol
25. Bessais B, Ezzaouia H, Bennaceur R (1993) Electrical behavior and optical properties of screen-printed ITO thin films. Semicond Sci Technol 8:1671–1678
26. Chang JF, Hon MH (2001) The effect of deposition temperature on the properties of Al-doped zinc oxide thin films. Thin Solid Films 386:79–86
27. Kim C, Park A, Prabakar K, Lee C (2006) Physical and electronic properties of ZnO:Al/porous silicon. Mater Res Bull 41:253–259
28. Ajimsha RS, Jayaraj MK, Kukreja LM (2008) Electrical characteristics of n-ZnO/p-Si heterojunction diodes grown by pulsed laser deposition at different oxygen pressures. J Electron Mater 37:357–365